CHEMICAL CHARACTERIZATION AND DITHIOTHREITOL REACTIVITY OF FINE PARTICULATE MATTER DERIVED FROM FOURTH GENERATION E-CIGARETTE USAGE

RACHEL LONG

A technical report submitted to the faculty at the University of North Carolina at Chapel Hill in partial fulfillment of the requirements for the degree of Master of Science in Public Health in the Department of Environmental Sciences and Engineering (Exposure Science) in the Gillings School of Global Public Health.

Chapel Hill

2017

ABSTRACT

Rachel Long: Chemical Characterization and Dithiothreitol Reactivity of Fine Particulate Matter Derived from Fourth Generation E-Cigarette Usage
Under the direction of Jason D. Surratt

Advanced electronic cigarettes, or advanced personal vaporizers (APVs), have larger battery capacities than older models, and allow greater user control of output wattage. It remains unclear how particle-phase composition and toxicity change as a function of wattage. This study physically and chemically characterized particle-phase constituents in APV emissions derived from typical e-liquid vehicles propylene glycol (PG) and glycerol (VG) at varying wattages. APV emissions were injected into a 1-m^3 Teflon chamber to measure real-time particle size distributions and to collect fine particles for offline chemical analyses and determination of their oxidative potential using the acellular dithiothreitol assay. Higher particle numbers were present at higher wattages, with the majority being < 100 nm. Particle-phase composition was dominated by VG at all wattages, with many low-abundance polyols also present, suggesting gas-phase radical chemistry. APV-derived particles have lower oxidative potentials compared to other particle types such as diesel exhaust and secondary organic aerosol.

ACKNOWLEDGEMENTS

First, I would like to acknowledge and thank my advisor, Professor Jason Surratt, for his guidance and support. His supervision was invaluable, and his positive attitude and infectious enthusiasm made the challenges and obstacles surmountable.

I also thank my committee members, Professors Barbara Turpin and Ilona Jaspers, for lending their expertise to this project. Their insights pushed me to consider new directions that elevated the study considerably. In addition, I thank Professor Ken Sexton, who was also very helpful in the early stages of the project.

My labmates in the Surratt and Turpin labs patiently answered my many questions throughout this process and often went out of their way to lend a helping hand. Thank you to Maiko Arashiro, Thais Barbosa, Yuzhi Chen, Tianqu Cui, Liyong Cui, Sara Duncan, Hilary Green, Grace Nipp, Hang Nguyen, Sarah Petters, Weruka Rattanavaraha, Caitlin Rose, Sophie Tomaz, Marc Webb, Mike Williams, Zhexi Zeng, and Yue Zhang. Special mention goes to Yuzhi Chen, Tianqu Cui, Hilary Green, and Weruka Rattanavaraha for devoting considerable time to teaching me the methods needed for my experiments and analyses.

I would also like to thank Leonard Collins in the Biomarker Mass Spectrometry Facility, whose expert knowledge helped the project go much more smoothly, and Phillip Clapp from the Curriculum in Toxicology, who assisted greatly in the conception of the study.

I would also like to acknowledge the funders of this study, the Tobacco Center of Regulatory Science (TCORS) at the University of North Carolina at Chapel Hill.

Finally, I extend gratitude to my partner, Kevin Li, for his love and encouragement, and for many home-cooked dinners and rides home from late nights in the lab. I also thank the Li/Chen family for their support and for making Chapel Hill feel like home. Emotionally and logistically, they all made this project possible.

TABLE OF CONTENTS

LIST OF TABLES AND FIGURES

Introduction

Electronic cigarettes (e-cigarettes, e-cigs) are increasingly popular worldwide as alternative nicotine delivery systems. In the U.S., 3.7% of adults currently use e-cigs, with this proportion being higher (20.3%) among smokers who had attempted to quit smoking (Schoenborn and Gindi, 2015). Among never-smokers, 3.2% of adults had ever used an e-cig (Schoenborn and Gindi, 2015). Also in the U.S., 24% of high school students reported using e-cigs in the 30 days prior to a 2015 survey, compared to only 11% of students who use conventional tobacco cigarettes (Centers for Disease Control and Prevention, 2016). E-cigs are a public health conundrum, as there is debate about whether the risks they pose to human health outweigh their usefulness as a smoking cessation device (CDC, 2015). They may cause public health harm if they lead to adoption of nicotine with other tobacco products by youth and current tobacco non-users, lead former smokers to relapse, or delay smoking cessation among current smokers. They also may cause public health harm if they result in nicotine poisonings or expose non-users to secondhand vapor. However, they may yield a net public health benefit if they help smokers transition completely from combustible tobacco products and transition society to overall low tobacco use (CDC, 2015).

In general, e-cigs have four main components: a mouthpiece, a cartridge or tank, an atomizer, and a battery. To activate the atomizer, the user either inhales through the mouthpiece to activate a sensor, or pushes a manual button that turns on the atomizer. The atomizer then heats up the e-liquid, or e-juice, stored in the device's cartridge or tank to produce a smoke-like aerosol that is then orally inhaled.

E-cigs are loosely grouped into four main categories, or generations. The first generation of e-cigs, or "cig-a-likes", physically resemble conventional tobacco cigs, have the least powerful batteries, which can be disposable or rechargeable, and their atomizers are activated via inhalation. Second-generation e-cigs, or "vape pens," have larger-capacity batteries than cig-a-likes, generally

have refillable e-liquid tanks or replaceable e-liquid cartridges, and typically require manual activation of the atomizer. The atomizers often come with a 510 threaded connection that allows users to switch out compatible atomizers or clearomizers that yield different effects on cloud production, flavor, or tank capacity. Third-generation e-cigs, called "advanced personal vaporizers" or APVs, are almost all operated via manual atomizer activation, and feature a "mod" or computerized power source. Mods fall into two categories, mechanical mods and regulated mods. Mechanical mods are simple by design and consist of the fire button, a battery compartment, and a connector for the atomizer. Because of this, they are more dangerous, as users must have thorough knowledge of electricity to be able to safely adjust the power (watts), resistance (ohms), and current (amps) of the device to their preference. Regulated mods are more complex but more user-friendly, as they have hardware that allows users to control device voltage and/or wattage output and include safety features such as resistance meters. Both types of mods can be user-modified and paired with a wide variety of atomizers or clearomizers, which can be purchased from a manufacturer ready-to-use, or custom-built by the user. Fourth generation e-cigs, also considered APVs, are the most powerful device type currently on the market and are distinguished from third-generation devices by additional customizable features such as low or sub-ohm coil resistances, adjustable airflow slots, and automatic temperature control settings that cap atomizer temperatures at a user-specified maximum.

There is a vast diversity of e-cig devices on the market, with over 460 brands available in 2014 and an estimated net increase of 10.5 brands added per month (Zhu et al., 2014). There is an even greater diversity of e-liquids, with 7764 e-liquid flavors on the market and 242 new flavors coming on to the market each month (Zhu et al., 2014). Most e-liquids consist of a vehicle of some close ratio of propylene glycol (PG) and vegetable glycerin (also called glycerol) (VG) to which

nicotine, flavorings, and other additives are added, and many e-liquids contain nicotine in varying concentrations up to 24 mg mL−1 (Dinakar and O'Connor, 2016). As such, e-cigs present a challenge to toxicologists, epidemiologists, health behavior scientists, and regulators, as the vast diversity of devices, e-liquids, device and e-liquid combinations, and user-adjusted settings lends yet more uncertainty to their net public health effect.

An important data gap in this debate is full chemical characterization of e-cig vapor, which can consist of compounds generated in both the gas and aerosol (particle) phases from a wide variety of e-liquids or e-juices. With regard to chemical composition of e-cig derived particles, most studies have focused on identification of toxic carbonyls, aldehydes, and other volatile organic compounds. The prevailing hypothesis for the generation of these toxic compounds is the thermal decomposition of PG and/or VG, as evidenced by several studies (Geiss et al., 2016; Gillman et al., 2016; Jensen et al., 2017; Sleiman et al., 2016). Several studies have tested devices across wattage settings and found generally increasing levels of toxic compounds such as acrolein, acetaldehyde, and formaldehyde with increased device wattage (Gillman et al., 2016; Husari et al., 2015; Khlystov and Samburova, 2016; Wang et al., 2017). However, few studies have examined particulate composition at the wattages that newer APV models can reach. Gillman et al. (2016) examined devices across a wattage range of 0.5-25 W, which constitutes the widest power setting range yet studied (Gillman et al., 2016). To date, no studies have yet characterized emissions from devices such as APVs that are capable of outputs of up to 100 watts. A 2017 review of eight recent survey studies on e-cigarette usage indicated that among 2,166 adolescent and young e-cigarette users, reported primary usage of later-generation devices ranged from 58% to 86% across studies, with an overall mean of 77.0% (95%CI: 70.5%, 82.9%) (Barrington-trimis et al., 2017). A 2016 study of e-cigarette design

preference and smoking cessation found that 41.1% of e-cigarette users reported using only modifiable, later-generation systems, with 7.4% of those surveyed reporting using both early-generation and later-generation systems (Chen et al., 2016). Though to date there are, to our knowledge, no peer-reviewed studies of e-cigarette user setting preferences on third- and fourth-generation devices, anecdotal evidence from user forums, such as those on Reddit, indicates that some users do use e-cigarettes at wattages up to or above 100 W (YahMezSoup, 2016).

The generation of reactive oxygen species (ROS) and the induction of oxidative stress is a strongly supported mechanism for the respiratory effects of numerous respiratory toxicants, including ambient aerosols (particles) (Pope, 2000; Reuter et al., 2010). ROS are highly chemically reactive oxidants such as the hydroxyl radical, super-oxide anion, and hydrogen peroxide that cause cell damage. The generation of ROS in airway epithelial cells and macrophages initiates a series of events that can lead to apoptosis and inflammation, which may contribute to clinically observable health outcomes (Glasauer and Chandel, 2013). Several recent *in vitro* studies have linked e-cig derived aerosols to oxidative stress (Rubenstein et al., 2015), including a study that observed significant oxidative stress in cells exposed to only the aerosolized base liquids, PG and VG as opposed to e-liquids with more complex mixtures of nicotine and flavorings (Scheffler et al., 2015).

The aim of this study was to examine the effect of device wattage on e-cig particulate composition. It is hypothesized that higher wattage settings on the same device will result in higher coil temperatures and thus greater thermal decomposition of the e-liquid and higher concentrations of toxic decomposition byproducts. This study exclusively examines a pure PG-VG "vehicle" liquid that reflects the majority of the mass of most e-liquids (Dinakar and O'Connor, 2016; Sleiman et al., 2016). The dithiothreitol (DTT) assay is an acellular assay frequently used to

quantify the oxidation of sulfides as a proxy measurement for the potential of a particulate sample to generate ROS (Li et al., 2009).This study also uses the DTT assay to measure the oxidative capacity of the compounds in APV-derived fine particles by determining the rate of oxidization of DTT to its disulfide form. APV-derived particles were chemically characterized from air filters using gas chromatography interfaced mass spectrometry (GC/MS) with prior trimethylsilylation and ultra- performance liquid chromatography (UPLC) coupled in-line to both a diode array detector (DAD) and high-resolution quadrupole time-of-flight mass spectrometry equipped with electrospray ionization source (ESI-HR-QTOFMS). As the first study, to our knowledge, to chemically characterize e-cig particulate composition from APVs at the higher end of available wattage settings, and the first known study to apply the DTT assay to e-cig particles, this work contributes to important data gaps in the e-cig literature.

Methods

Chemicals, E-Liquids, and Vaporizers

The device used for experiments was a Sigelei 150 W TC mod with SMOK TFV4 Mini stainless steel and 5 mL glass tank best described as a clearomizer, as it allows the user to see the liquid inside and the atomizer is housed within the tank. A TF-S6 coil head was used inside the tank (kanthal coil, organic cotton wick, 0.35 ohm resistance, 30-100 W range). No modifications were made to the coils or to the device. The device had two sets of vents on the tank component. All experiments were performed with the top side vents (closest to the mouthpiece) completely closed and the side vents on the bottom of the device completely open. Efest 18650 batteries powered the device and were fully charged before all experiments. The e-liquid was formulated using a 1:1 ratio of lab-grade PG (Sigma Aldrich, 99.5%) and VG (Sigma Aldrich, 99.5%).

Vapor Generation

The device was connected to a 1-m^3 Teflon chamber with two Teflon ports, one for injection and one for sampling. The chamber was purged with clean house air for 2.5 hours before each experiment to allow four chamber volumes of air to circulate. Background chamber particle concentrations were determined before each experiment from the sampling port using a differential mobility analyzer (DMA, Brechtel Manufacturing, Inc., Model 2002) coupled to a mixing condensation particle counter (MCPC, Brechtel Manufacturing, Inc., Model 1710). Real-time temperature and relative humidity (RH) of the chamber was taken from the injection port during all experiments using a USB RH and Temperature Sensor (Omega Engineering, Inc.). The mean RH and temperature in the chamber in the 10 min preceding injection of APV emissions was 10.8% (range was from 7.5 - 14.8%) 23.2 °C (range was from 22.8 - 24.5 °C), respectively. Experiments were initiated when the background particle mass concentration of the chamber was less than 1 µg m^{-3}. This background particle mass concentration assumes unit density, a reasonable assumption, as the densities of PG and VG are 1.04 g/cm³ and 1.26 g/cm³, respectively.

The APV vapors and particles were injected into the chamber via the following process: (1) the device was connected via non-conductive tubing to a Venturi eductor (Jacobs Analytics), which in turn was connected to the chamber using stainless steel Swagelok connectors (Swagelok); (2) the device was fired for 10 seconds and the APV emissions drawn into the chamber at 2 LPM via the Venturi eductor; (3) immediately after firing the APV device, the inlet of the chamber was re-sealed with the RH and temperature probe; and (4) the clearomizer and tank component of the APV device was weighed before and after each injection to get the mass of e-liquid consumed during each experiment.

Filter Sampling

After injection of APV emissions, particle mass concentrations inside the chamber were continuously monitored using the DMA-MCPC system until they stabilized. Upon stabilization of the chamber particle mass concentration, filter sampling was initiated. Two pre-weighed Teflon filters (2 μm pore size, 37 mm, Pall Life Sciences) were added to a $PM_{2.5}$ filter sampler. The average sampling flow rate was 10 LPM, and was generated by a vacuum pump. Flow rates were measured before and after each sampling event. Filters were weighed immediately after sampling and stored in separate 20 mL borosilicate vials under dark and -20 °C conditions until chemical analyses.

Offline Chemical Analysis

Filters were extracted by 45 min of sonication in 20 mL of methanol (LC-MS Chromasolv®, 99.9%, Fisher) in 20 mL borosilicate vials. Aliquots of the extractions were separated for the different types of analyses (GC/MS, UPLC/DAD-ESI-HR-QTOFMS, DTT assay) and also stored in borosilicate glass vials. Extractions were stored under dark conditions in a -20 °C freezer when not in use.

Filter extracts were dried under nitrogen (N_2) gas using an N_2 evaporator (Thermo Electron) for up to 6 h. For GC/MS analyses, resultant organic residues were trimethylsilylated with 100 μL of BSTFA (N,O-bis(trimethylsilyl)trifluoroacetamide) and TMCS (trimethylchlorosilane) (99:1 v/v, Supelco) and 50 μL of pyridine (anhydrous, 99.8%, Sigma Aldrich) at 70 °C for 1 h. 1 μL aliquots of each trimethylsilylated sample were injected onto an Econo-Cap™-EC™-5 capillary column (30 m x 0.25 mm I.D.; 0.25 mm film thickness) to separate the e-cig particle-phase constituents before MS detection in a Hewlett-Packard (HP) 5890 Series II gas chromatograph, which is coupled to a HP 5971A Mass Selective Detector (MSD). The

analytical procedures and the instrumental operating conditions have been described in detail previously (Surratt et al., 2010)

Another portion of filter extractions were used for UPLC/DAD-ESI-HR-QTOFMS analyses. After filter extracts were dried, resultant organic residues were reconstituted in 150 µL of 50:50 (v/v) solvent mixture of methanol (LC-MS CHROMASOLV-grade, Sigma-Aldrich) and water). UPLC/DAD-ESI-HR-QTOFMS was performed using an Agilent 6500 series system equipped with a Waters Acquity UPLC HSS T3 column (2.1×100mm, 1.8µm particle size). Detailed operating conditions for the UPLC/DAD-ESI-HR-QTOFMS have been previously described (Riva et al., 2016; Zhang et al., 2011).

DTT Assay

Calibration curves using DTT and the known DTT oxidant 1,4-naphthoquinone (1,4-NQ) were generated to measure DTT consumption by the APV products (Figures 1a and 1b). First an aqueous buffer solution of 0.1 M potassium phosphate monobasic-sodium hydroxide (KH_2PO_4, pH 7.4, Fisher Scientific) and 1 mM ethylenediaminetetraacetic acid (EDTA, Sigma Aldrich) was prepared. A fresh stock solution of 5 mM DTT standard was prepared daily before each assay by adding 7.712 mg of the DTT standard powder to 10 mL of the buffer solution. A 10 mM 5,5'-dithiobis-(2-nitrobenzoic acid (DTNB) stock solution was made by dissolving 19.817 mg DTNB in 5 mL buffer. A stock solution of 1,4-NQ was prepared with 0.5 mg of 1,4-NQ dissolved into 0.5 mL dimethyl sulfoxide (DMSO). Working solutions of 0.05 mM DTT, 1 mM DTNB, and 0.01 1,4-NQ were made by diluting the stock solutions with the buffer solution. All solutions were made in clear borosilicate glass vials.

To generate calibration curves, varying amounts of standard solutions and the 1,4-NQ external standard were added to the reaction vial. For sample analysis, 100 - 300 µg of extracted

e-cig aerosol in 100 µL methanol was added to the reaction vial. The reactants were incubated at 37 °C for 30 min and quenched immediately afterward by adding 100 µL of the 1 mM DTNB working solution. Within 2 h of quenching, the absorbance of the product formed by the oxidation of the remaining DTT with the DTNB, 5-thio-2-nitrobenzoic acid (TNB), was measured at 412 nm using UV-Visible Spectrophotometer (Hitachi U-3300 dual beam spectrophotometer). Previous studies by our group have determined that the order of reagent addition, the presence of methanol in the sample extract, and the presence of DMSO do not affect assay results (Kramer et al., 2015).

The DTT consumption of the APV-derived particulate samples was calculated from their absorbance using the calibration curves and the following formulas:

$$\mathrm{IOG} = \frac{\mathrm{Abs}_0 - \mathrm{Abs}'}{\mathrm{Abs}_0} \times \frac{100}{\mathrm{T} \times \mathrm{M}} \qquad [1]$$

$$\mathrm{NIOG}_{\mathrm{sample}} = \frac{\mathrm{IOG}_{\mathrm{sample}}}{\mathrm{IOG}_{1,4-\mathrm{NQ}}} \qquad [2]$$

The index of oxidation generation (IOG) is calculated using equation [1] where Abs_0 is the initial absorbance (at 0 min), Abs' is the absorbance at time T for a given sample, T is the reaction time in min, and M is the mass of the sample (µg). The NIOG is calculated by taking the ratio of the IOG of the sample of interest and the IOG for the 1,4-NQ known oxidant (equation [2]).

The DTT consumption was expressed as the NIOG for purposes of comparison with previous studies by our group (Kramer et al., 2015; Rattanavaraha et al., 2011). One-way analysis

of variance (ANOVA) followed by t-tests were used to test the significance of differences among the wattage settings.

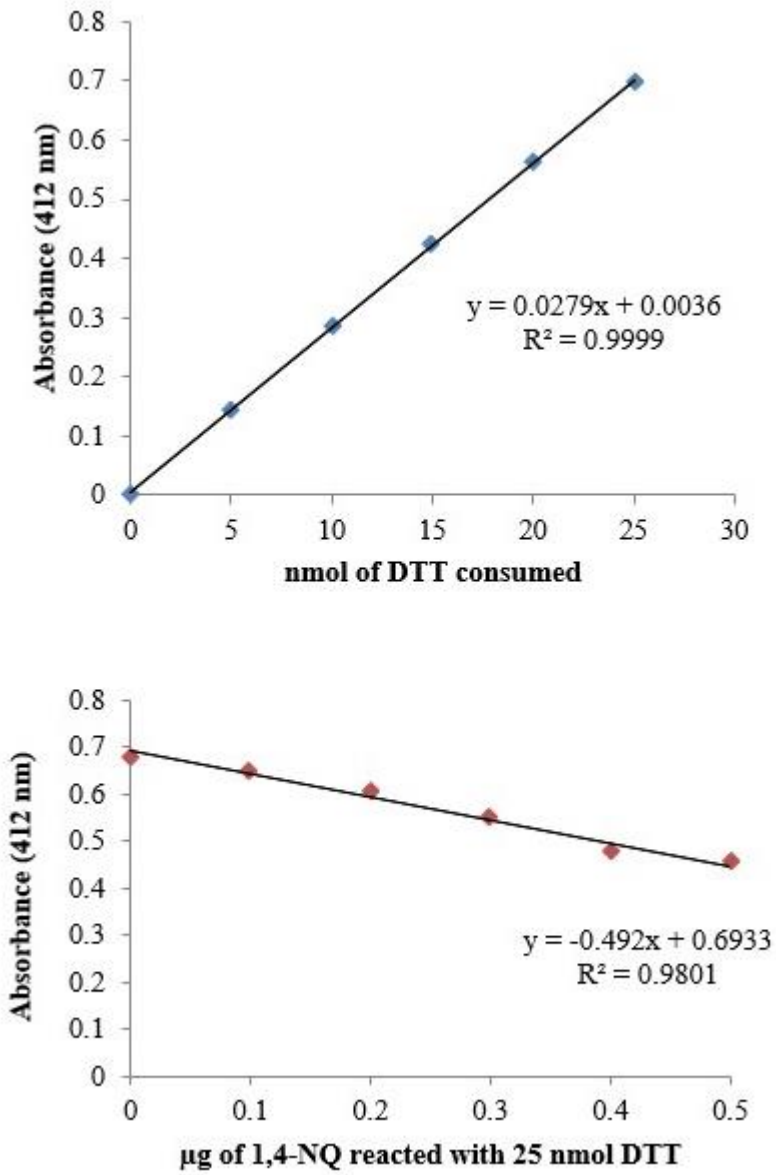

Figure 1. Calibration curves for the measured absorbance of TNB versus (a) nmol of DTT consumed and (b) various masses of 1,4-NQ reacted with 25 nmol DTT.

Results and Discussion

E-liquid Consumption and Aerosol Generation

E-liquid consumption increased with increasing wattage setting (Figure 2). The 40-watt setting was significantly different from all other settings and the 60-watt setting was significantly different from the 80-watt setting ($p<0.05$). Filter mass collected on the upstream filter during sampling also generally increased with increasing wattage setting, with the exception of the 80-watt setting (Figure 3). In terms of the filter mass collected, the 100-watt setting was significantly different from all other settings. The upstream filter was highly efficient: the mass of the downstream filters in all experiments was 0.1-1% of that of the upstream filters. The downstream filters were thus not chemically characterized or used for DTT analyses.

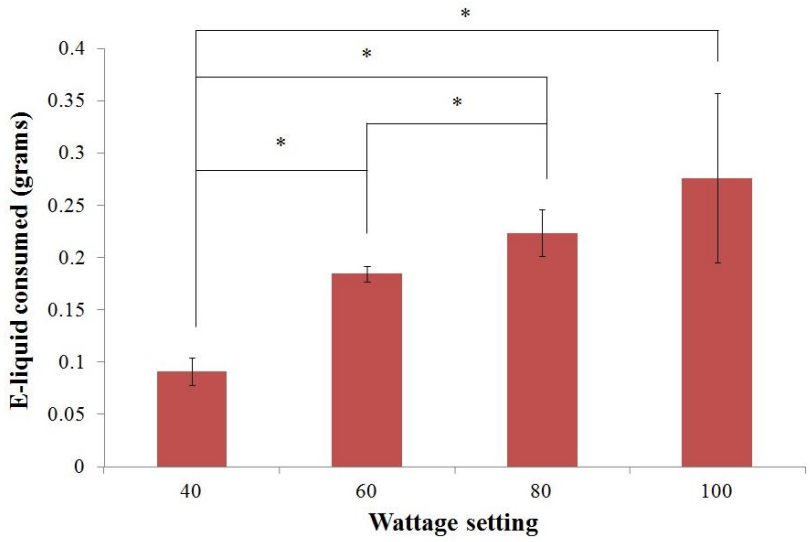

Figure 2. E-liquid consumed per ten-second puff at 40, 60, 80, and 100 watt APV settings (n=3 per setting).

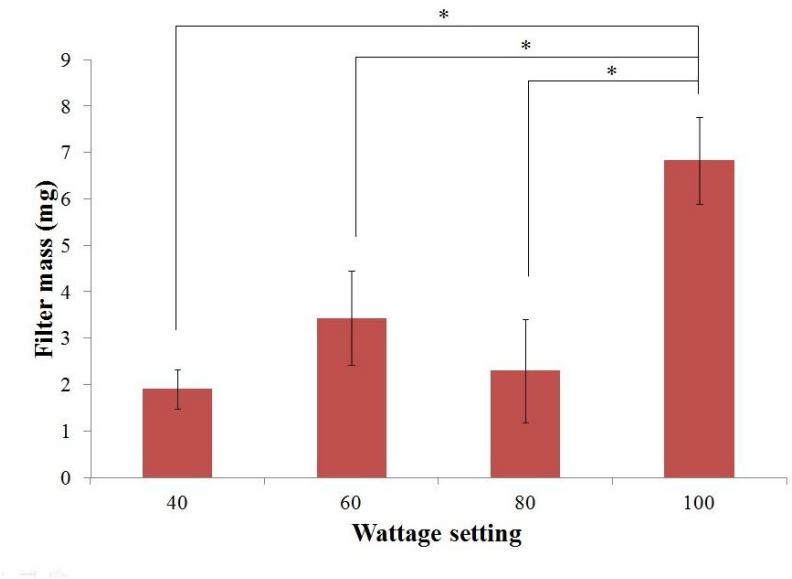

Figure 3. Aerosol mass collected per sampling period per ten-second puff at 40, 60, 80, and 100 watt APV settings (n=3 per setting).

Particle Sizing

Particle size distribution in terms of particle number are plotted below in Figure 4. At all settings, the distributions followed a bimodal size distribution, with higher particle number concentrations in the nucleation mode (< 100 nm particle diameter). In general, increasing particle number concentrations with increasing wattage were observed in the chamber, with the exception of the 80 watt setting, which had a lower particle number concentration than the 60 watt setting at most particle sizes (Figure 4). Particle sizing data indicates particles in the ultrafine size range (<100 nm), which have been shown in ambient air pollution studies to have more severe health effects than larger particles (Delfino et al., 2005). The size distributions suggest nucleation via supersaturation of low-volatility products as the primary mechanism for aerosol formation, though it is possible that condensation on pre-existing particles in the chamber or heterogeneous nucleation with metals from the heating of the kanthal coil could be responsible.

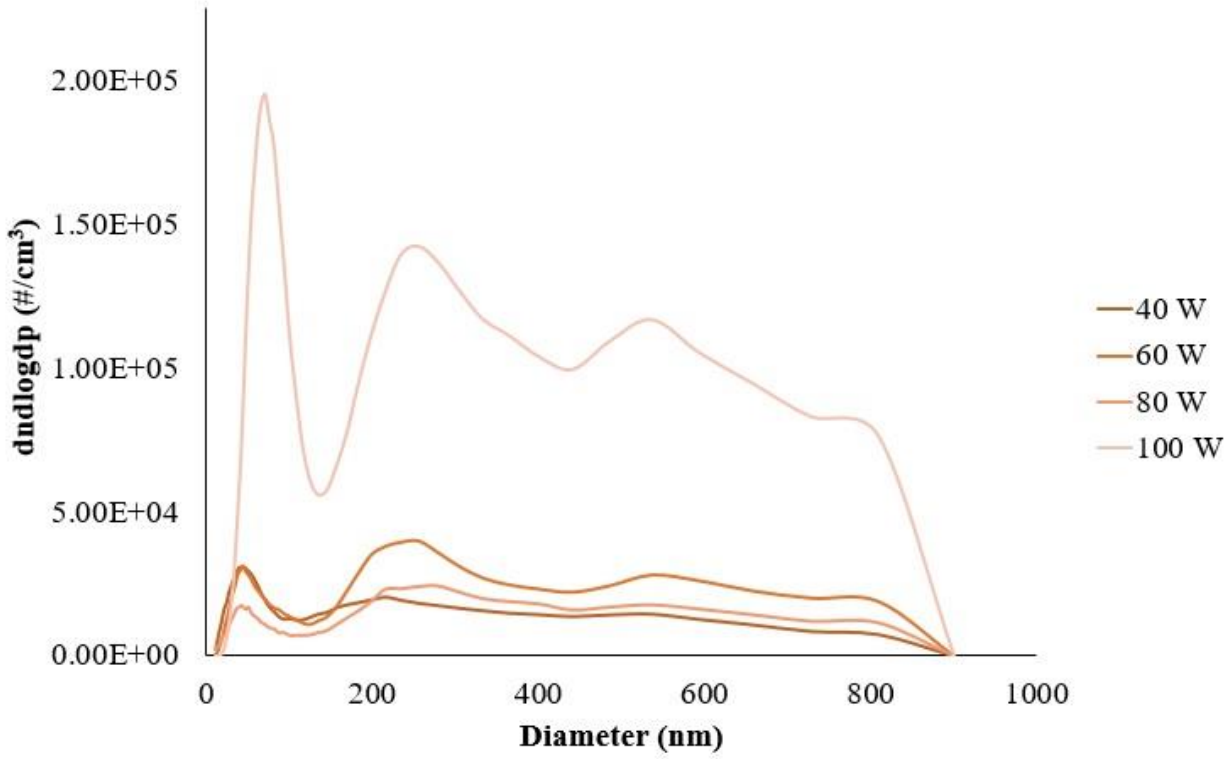

Figure 4. Stabilized aerosol particle number size distributions in chamber per sampling period per ten-second puff at 40, 60, 80, and 100 W settings (n=1 per setting).

GC/MS Analysis

The GC/MS total ion chromatograms (TICs) for APV aerosols produced in the 1-m^3 Teflon chamber are shown in Figures 5, 6, and 7. The abundance of the dominant glycerol peak, visible at retention time ~22 min, increased with increasing wattage setting (Figure 5). Peaks representing less-abundant compounds were visible between retention times 24 and 56 minutes, and appeared to differ in abundance between different wattage settings (Figure 6). Among replicates of filters from the same wattage setting, the abundances of the less-abundant

compounds appeared to be consistent compared to their abundances across different wattage settings (Figure 7).

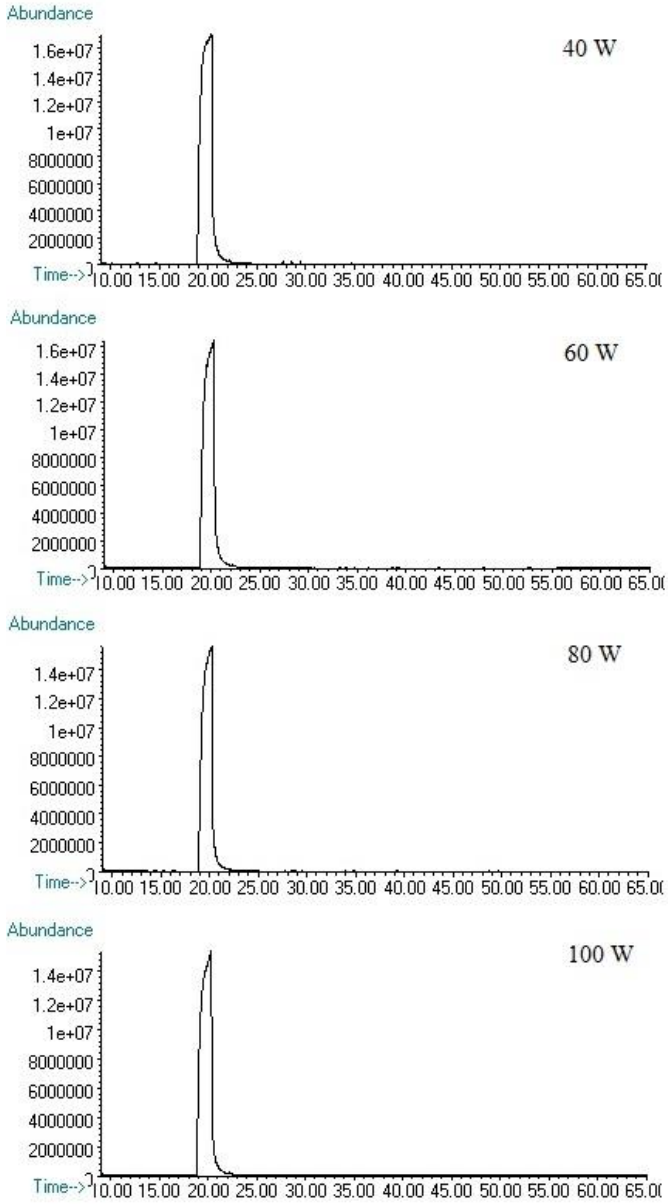

Figure 5. GC/MS TICs for 40, 60, 80, and 100 watt condition filter samples (retention times 0-65 min).

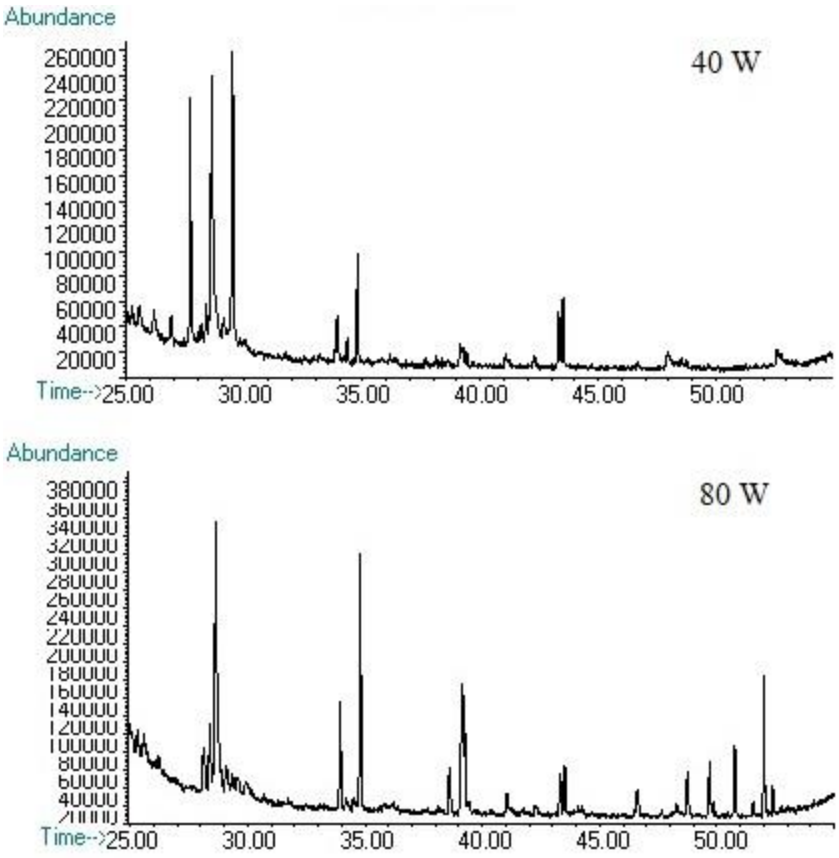

Figure 6. GC/MS TICs for 40 and 80 watt condition filter samples from retention times 24-56 min.

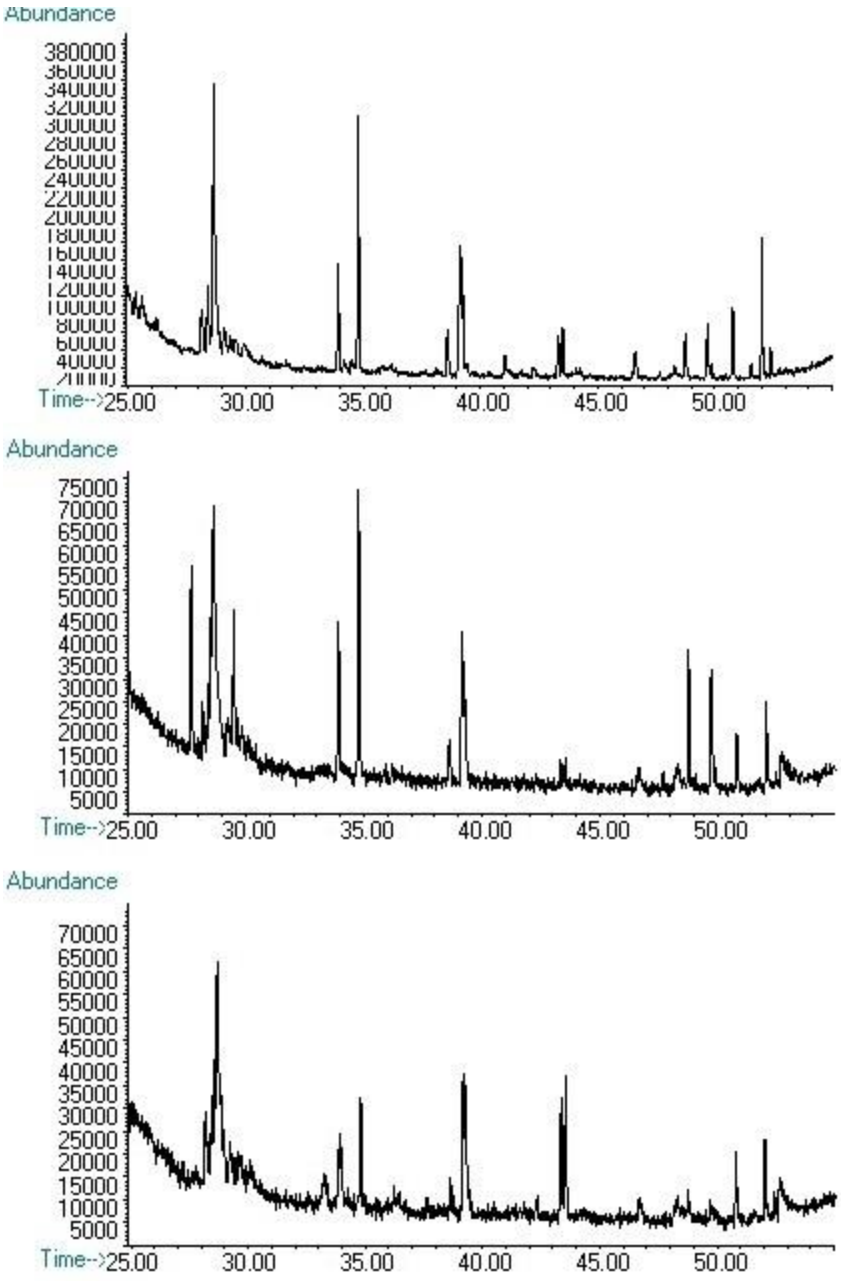

Figure 7. GC/MS TICs three replicates of 80 watt condition filter samples from retention times 24-56 min.

UPLC/DAD-ESI-HR-QTOFMS Analysis

The positive ion mode UPLC/DAD-ESI-HR-QTOFMS TICs for APV-derived particles produced in the 1-m^3 Teflon chamber are shown in Figure 8. Oligomer composition of the aerosol appear to differ by wattage setting. The full list of compounds identified using positive ion mode data are listed in Table 1. Among the possible molecular formulas suggested by the LCMS software, the molecular formula with the lowest mDa difference for each mass was included in the table. To be included in the table, the compound's abundance had to be at least four orders of magnitude higher than the baseline for a given sample. Suggested compounds containing nitrogen, sulfur, or other non-hydrocarbons were not included. Average abundances of identified compounds by wattage setting normalized by filter mass are shown in Figure 9. Glycerol ($C_3H_8O_3$) is the most abundant compound at every setting, yet makes up a smaller proportion of the mass of the 100 W aerosols on average. Some of the less-abundant compounds appear to be simple oligomers of PG and/or VG, while other polymers may be explained by radical chemistry, which has been observed in recent studies of e-cigarette aerosols (Goel et al., 2015).

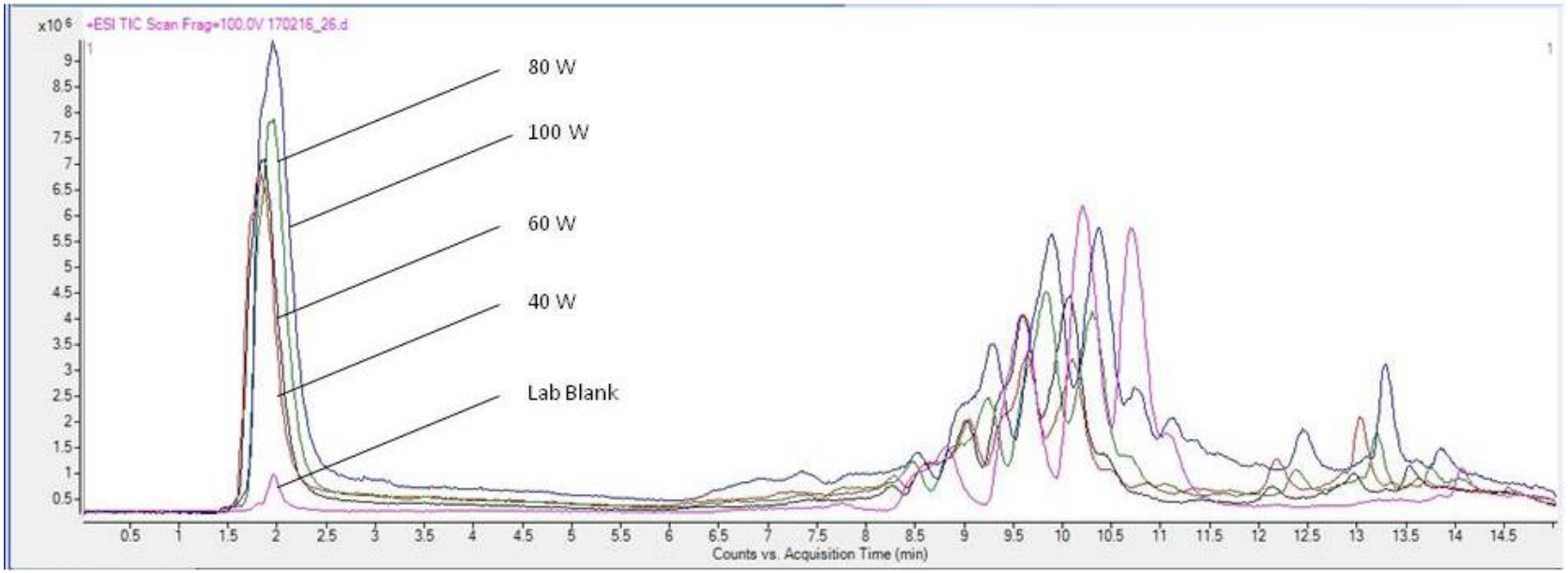

Figure 8. Overlay of positive ion mode LC/MS TICs from 40, 60, 80, and 100 watt conditions and lab blank filter sample; n=1 for each wattage condition and lab blank.

							Sample Number (Wattage-Replicate Number)											
Calc m/z	Retention Time	Mass	Formula (M)	Diff (ppm)	Diff (mDa)	Double Bond Equivalents	40-1	60-1	80-1	100-1	40-2	60-2	80-2	100-2	40-3	60-3	80-3	100-3
149.0209	13.923-14.338	126.033	C6 H6 O3	-10.06	-1.27	4	0	1,263	0	0	0	0	40,129	0	0	0	869	85,891
177.0522	13.692-13.858	154.0642	C8 H10 O3	-7.85	-1.21	4	0	100,968	0	178,422	168,819	289,504	793,548	143,903	847,069	452,292	388,503	621,414
115.0366	1.577-2.290	92.0479	C3 H8 O3	-5.58	-0.51	0	6,686,632	7,056,220	5,859,848	4,324,413	5,995,532	6,641,012	9,455,439	1,715,154	6,268,371	6,467,279	9,161,662	5,728,651
181.026	1.330-1.645	158.0366	C10 H6 O2	1.29	0.2	8	0	0	0	0	8,426	0	0	0	0	0	0	0
183.1356	12.063-12.229	160.1481	C9 H20 O2	-10.94	-1.75	0	0	350,733	339,013	270,589	623,525	262,114	430,023	78,003	349,027	342,990	373,192	234,561
189.0733	1.622-2.319	166.0834	C6 H14 O5	4.27	0.71	0	0	0	0	0	0	0	0	165,078	0	0	0	0
203.089	7.310-7.542	180.099	C7 H16 O5	4.19	0.76	0	86,025	167,945	0	351	0	947	177,516	32,200	158,599	164,875	106,840	250
205.0835	13.459-13.592	182.0956	C10 H14 O3	-6.95	-1.26	4	0	666	25,276	1,174	0	0	203,953	36,996	0	113,604	0	520
217.1046	8.299-9.180	194.1148	C8 H18 O5	3.13	0.61	0	1,107	294,658	0	0	0	0	0	0	0	0	0	0
223.0941	13.457-13.689	200.1067	C10 H16 O4	-9.36	-1.87	3	288,412	91,613	292,965	158,399	148,881	247,494	646,115	117,201	758,444	363,046	344,925	494,558
245.0784	13.371-13.554	222.0882	C12 H14 O4	4.35	0.97	6	1,788,655	7,863	71,300	0	0	0	174,970	0	157,462	0	1,238	0
255.1203	11.961-12.143	232.1342	C11 H20 O5	-13.43	-3.12	2	839	85,085	786	0	0	0	0	0	9,857	0	107,726	0
257.1359	12.909-13.025	234.1491	C11 H22 O5	-10.24	-2.4	1	0	0	803,973	0	0	0	0	0	785,325	0	0	0
259.0788	7.310-7.542	236.0898	C9 H16 O7	-0.79	-0.19	2	2,258	0	0	0	0	0	1,914	0	0	0	0	0
259.2032	12.063-12.229	236.2116	C16 H28 O	10.2	2.41	3	0	0	0	0	0	0	1,377	0	0	0	0	0
261.1309	9.178-9.393	238.1416	C10 H22 O6	0.14	0.03	0	0	0	0	0	0	0	950,508	0	0	0	0	0
268.9998	1.755-19.71	246.0086	C19 H2 O	8.12	2	19	144,161	0	0	30,875	0	608	0	10,686	0	0	0	6,441
279.1203	12.909-13.025	256.1317	C13 H20 O5	-2.51	-0.64	4	754,041	0	0	1,056,910	0	1,170,543	0	224,761	0	0	0	1,200,273
279.1567	13.923-14.340	256.1696	C14 H24 O4	-8.37	-2.14	3	0	0	0	0	0	0	0	0	0	0	0	100,822
301.141	13.635-14.133	278.1525	C16 H22 O4	-2.4	-0.67	6	4,579,431	0	0	0	0	0	0	0	0	0	0	44,280
309.1309	12.063-12.229	286.1431	C14 H22 O6	-5.21	-1.49	4	231,768	0	0	0	0	0	0	0	0	0	0	0
433.0014	1.755-19.73	410.015	C16 H10 O13	-6.99	-2.86	12	0	0	0	0	0	0	0	0	0	0	0	126,889
459.49	13.692-13.863	436.4986	C31 H64	5.13	2.24	0	0	0	0	0	0	0	0	0	0	0	0	100
535.2514	12.909-13.025	512.263	C26 H40 O10	-1.62	-0.83	7	117,992	306,284	283,181	352,318	201,795	0	250,844	45,501	231,519	311,572	272,702	364,695
595.2725	12.437-12.652	572.2828	C28 H44 O12	0.88	0.5	7	0	0	0	14,684	0	0	0	66	0	0	0	14,592

Table 1. Compounds and their filter-mass normalized abundances for aerosol-phase APV samples as determined by positive ion mode LC/MS analysis.

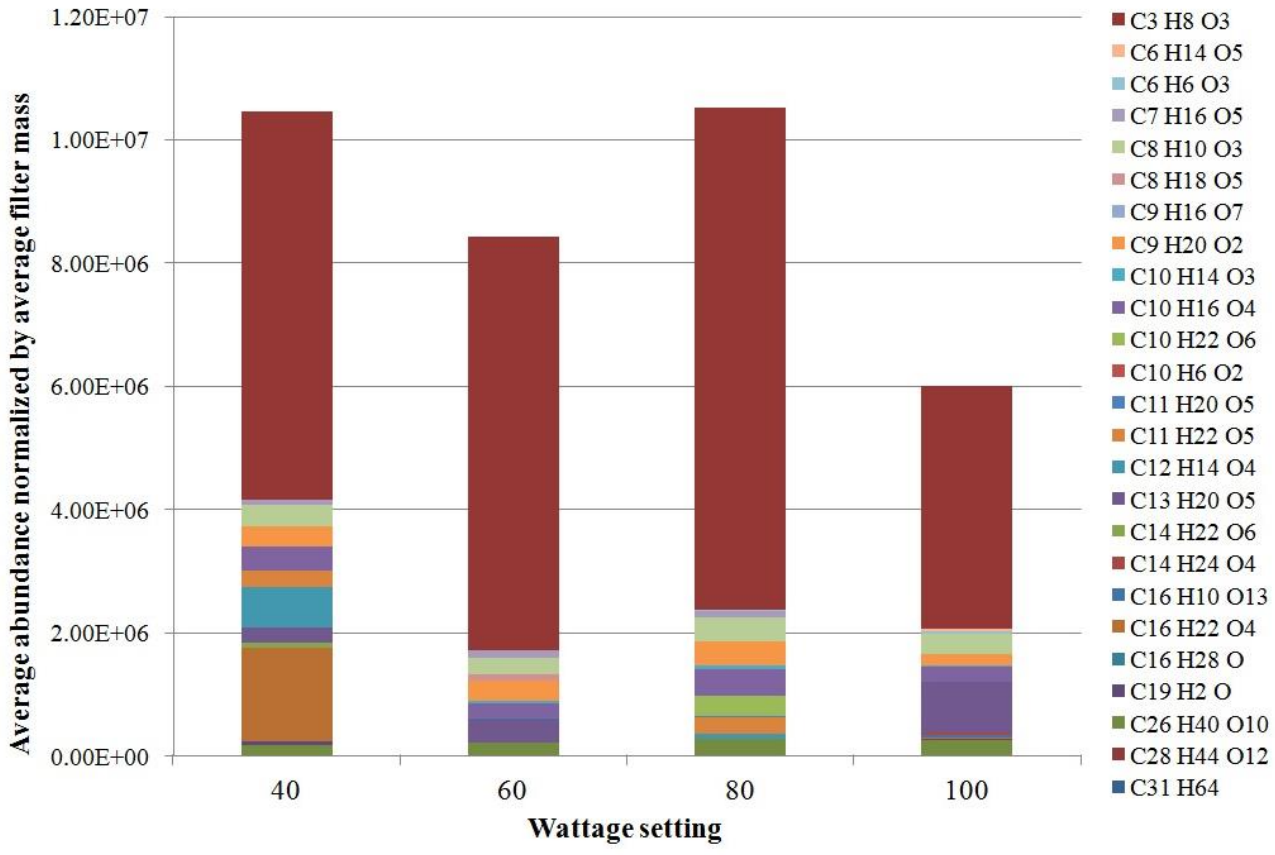

Figure 9. Plot of compounds with molecular formulas identified by UPLC/DAD-ESI-HR-QTOFMS operated in the positive ion mode in terms of average filter-mass normalized abundance by wattage setting.

DTT Assay

The DTT assay was conducted using three filter samples at each wattage condition and three samples each of neat PG, neat VG, and a 50:50 mixture of PG and VG. The NIOG values for the four wattage conditions and the three standards were not statistically significantly different according to an ANOVA. The NIOG values presented in Figure 10 are lower than those observed in DTT assays of isoprene-derived epoxides and secondary organic aerosol (Kramer et al., 2016) and diesel exhaust particles (Rattanavaraha et al., 2011).

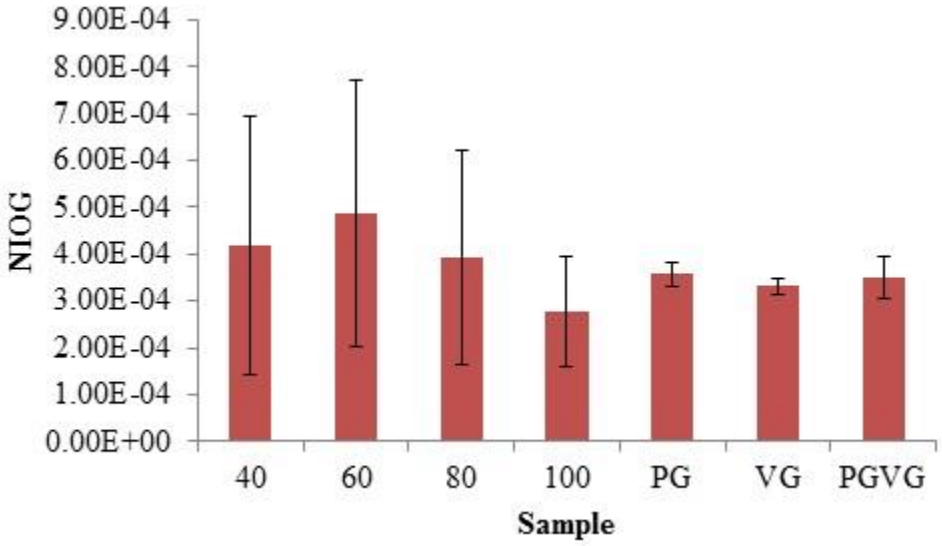

Figure 10. Normalized index of oxidant generation (NIOG) values for APV aerosol samples and standards tested for ROS generation using the DTT assay; n=3 for each setting and standard.

It is important to note that the DTT assay method used for this study involved the addition of a chelation agent, EDTA, which may render oxidative stress-inducing metals unreactive with DTT. The results therefore represent the oxidative stress potential of only the organic fraction of the e-cigarette aerosol. Prior work has shown heavy metals present in e-cigarette aerosols (Goniewicz et al., 2014; Saffari et al., 2014; Williams et al., 2013) and that transition metals induce

high DTT activities (Charrier and Anastasio, 2012). Future studies of e-cigarette aerosols involving the DTT assay may consider omitting the chelating agent. Though the DTT assay has correlated well with certain cellular oxidative stress assays (Li et al., 2003; Steenhof et al., 2011), it is often used as a relative rather than absolute measure of oxidative stress potential (Li et al., 2003). Recent studies indicating ROS activity of 50:50 PG:VG e-cig liquids (Lerner et al., 2015; Rubenstein et al., 2015; Scheffler et al., 2015) are difficult to compare to the DTT assay results of this study due to most of such studies using flavored e-liquids rather than the plain 50:50 PG:VG e-liquid vehicle.

Our study had several limitations. Though coil temperature is the parameter expected to be most influential in the generation of toxic thermal decomposition products, it is difficult to measure the actual temperatures reached by the e-cig coil, as it is enclosed in the e-liquid reservoir, which must be sealed during vaping. Puff topography varies according to user, and has a unique distribution that is challenging to mimic using machinery. Human upper respiratory system humidity is higher than that present in the ambient room conditions used in our study (Ruzer and Harley, 2004). Humidity may influence particle size distributions, as PG and VG are hygroscopic.

Future directions for this work include examining additional APV device settings and wider range of these settings. Puff topography has also been shown to have an effect on e-cig particle-phase composition (Cox et al., 2016; Zhao et al., 2016). Different e-liquid flavors, including those containing nicotine, should also be tested to see how some of the more benign and toxic flavors are altered as a result of vaporization at extremely high temperatures. Aging of the particles in the chamber may also provide some insight about the composition of second-hand emissions. In terms of analytical methods, real-time chemical characterization of the gas-

phase constituents from e-cig emissions will also be important in understanding the composition of the total inhaled vapor. Tandem MS (MS/MS) data is available from this dataset, which can help elucidate structures of the polymers identified using UPLC/DAD-ESI-HR-QTOFMS. Additional future work can include online mass spectrometry analyses using aerosol mass spectrometry or chemical ionization mass spectrometry. Analysis of APV aerosol samples using inductively coupled plasma mass spectrometry may characterize metals present in the aerosol that may result due to the heating of metal elements of the tank or kanthal coil, which may also influence DTT activity.

References

Barrington-trimis, J.L., Gibson, L.A., Halpern-felsher, B., Harrell, M.B., Kong, G., Krishnan-sarin, S., Leventhal, A.M., Loukas, A., Mcconnell, R., Weaver, S.R., 2017. Brief report Type of E-Cigarette Device Used Among Adolescents and Young Adults : Findings From a Pooled Analysis of Eight Studies of 2166 Vapers 1–4. doi:10.1093/ntr/ntx069

CDC, 2015. CDC Office on Smoking and Health E-cigarette Information. Cdc 1–2.

Centers for Disease Control and Prevention, 2016. Youth risk behavior surveillance — United States, 2015. Morb. Mortal. Wkly. Rep. 65, 3–4.

Charrier, J.G., Anastasio, C., 2012. On dithiothreitol (DTT) as a measure of oxidative potential for ambient particles: Evidence for the importance of soluble \newline transition metals. Atmos. Chem. Phys. 12, 9321–9333. doi:10.5194/acp-12-9321-2012

Chen, C., Zhuang, Y., Zhu, S., 2016. E-Cigarette Design Preference and Smoking Cessation. Am. J. Prev. Med. 51, 356–363. doi:10.1016/j.amepre.2016.02.002

Cox, S., Kośmider, L., McRobbie, H., Goniewicz, M., Kimber, C., Doig, M., Dawkins, L., 2016. E-cigarette puffing patterns associated with high and low nicotine e-liquid strength: effects on toxicant and carcinogen exposure. BMC Public Health 16, 999. doi:10.1186/s12889-016-3653-1

Delfino, R.J., Sioutas, C., Malik, S., 2005. Review Potential Role of Ultrafine Particles in Associations between Airborne Particle Mass and Cardiovascular Health 934–946. doi:10.1289/ehp.7938

Dinakar, C., O'Connor, G.T., 2016. The Health Effects of Electronic Cigarettes. N. Engl. J. Med. 375, 1372–1381. doi:10.1056/NEJMra1502466

Geiss, O., Bianchi, I., Barrero-Moreno, J., 2016. Correlation of volatile carbonyl yields emitted by e-cigarettes with the temperature of the heating coil and the perceived sensorial quality of the generated vapours. Int. J. Hyg. Environ. Health 219, 268–277. doi:http://dx.doi.org/10.1016/j.ijheh.2016.01.004

Gillman, I.G., Kistler, K.A., Stewart, E.W., Paolantonio, A.R., 2016. Effect of variable power levels on the yield of total aerosol mass and formation of aldehydes in e-cigarette aerosols. Regul. Toxicol. Pharmacol. 75, 58–65. doi:10.1016/j.yrtph.2015.12.019

Glasauer, A., Chandel, N.S., 2013. Ros. Curr. Biol. 23, 100–102. doi:10.1016/j.cub.2012.12.011

Goel, R., Durand, E., Trushin, N., Prokopczyk, B., Foulds, J., Elias, R.J., Richie, J.P., 2015. Highly Reactive Free Radicals in Electronic Cigarette Aerosols. Chem. Res. Toxicol. 28, 1675–1677. doi:10.1021/acs.chemrestox.5b00220

Goniewicz, M.L., Knysak, J., Gawron, M., Kosmider, L., Sobczak, A., Kurek, J., Prokopowicz, A., Jablonska-Czapla, M., Rosik-Dulewska, C., Havel, C., Jacob, P., Benowitz, N., 2014. Levels of selected carcinogens and toxicants in vapour from electronic cigarettes. Tob. Control 23, 133–9. doi:10.1136/tobaccocontrol-2012-050859

Husari, A., Shihadeh, A., Talih, S., Hashem, Y., El Sabban, M., Zaatari, G., 2015. Acute Exposure to Electronic and Combustible Cigarette Aerosols: Effects in an Animal Model and in Human Alveolar Cells. Nicotine Tob. Res. ntv169. doi:10.1093/ntr/ntv169

Jensen, R.P., Strongin, R.M., Peyton, D.H., 2017. Solvent Chemistry in the Electronic Cigarette Reaction Vessel. Sci. Rep. 7, 42549. doi:10.1038/srep42549

Khlystov, A., Samburova, V., 2016. Flavoring Compounds Dominate Toxic Aldehyde Production during E-Cigarette Vaping. Environ. Sci. Technol. acs.est.6b05145. doi:10.1021/acs.est.6b05145

Kramer, A.J., Rattanavaraha, W., Zhang, Z., Gold, A., Surratt, J.D., Lin, Y.H., 2016. Assessing the oxidative potential of isoprene-derived epoxides and secondary organic aerosol. Atmos. Environ. 130, 211–218. doi:10.1016/j.atmosenv.2015.10.018

Kramer, A.J., Rattanavaraha, W., Zhang, Z., Gold, A., Surratt, J.D., Lin, Y.H., 2015. Assessing the oxidative potential of isoprene-derived epoxides and secondary organic aerosol. Atmos. Environ. 130, 211–218. doi:10.1016/j.atmosenv.2015.10.018

Lerner, C.A., Sundar, I.K., Yao, H., Gerloff, J., Ossip, D.J., McIntosh, S., Robinson, R., Rahman, I., 2015. Vapors produced by electronic cigarettes and E-juices with flavorings induce toxicity, oxidative stress, and inflammatory response in lung epithelial cells and in mouse lung. PLoS One 10, 1–26. doi:10.1371/journal.pone.0116732

Li, N., Sioutas, C., Cho, A., Schmitz, D., Misra, C., Sempf, J., Wang, M., Oberley, T., Froines, J., Nel, A., 2003. Ultrafine particulate pollutants induce oxidative stress and mitochondrial damage. Environ. Health Perspect. 111, 455–460. doi:10.1289/ehp.6000

Li, Q., Wyatt, A., Kamens, R.M., 2009. Oxidant generation and toxicity enhancement of aged-diesel exhaust. Atmos. Environ. 43, 1037–1042. doi:10.1016/j.atmosenv.2008.11.018

Pope, C.A., 2000. Epidemiology of fine particulate air pollution and human health: Biologic mechanisms and who's at risk? Environ. Health Perspect. 108, 713–723. doi:10.1289/ehp.00108s4713

Rattanavaraha, W., Rosen, E., Zhang, H., Li, Q., Pantong, K., Kamens, R.M., 2011. The reactive oxidant potential of different types of aged atmospheric particles: An outdoor chamber study. Atmos. Environ. 45, 3848–3855. doi:10.1016/j.atmosenv.2011.04.002

Reuter, S., Gupta, S.C., Chaturvedi, M.M., Aggarwal, B.B., 2010. Oxidative stress, inflammation, and cancer: How are they linked? Free Radic. Biol. Med. 49, 1603–1616. doi:10.1016/j.freeradbiomed.2010.09.006

Riva, M., Bell, D.M., Hansen, A.K., Drozd, G.T., Allen, H., 2016. Effect of Organic Coatings , Humidity and Aerosol Acidity on Multiphase Chemistry of Isoprene Epoxydiols. doi:10.1021/acs.est.5b06050

Rubenstein, D.A., Hom, S., Ghebrehiwet, B., Yin, W., 2015. Tobacco and e-cigarette products initiate Kupffer cell inflammatory responses. Mol. Immunol. 67, 652–660. doi:10.1016/j.molimm.2015.05.020

Ruzer, L.S., Harley, N.H., 2004. Aerosols Handbook: Measurement, Dosimetry, and Health Effects, Second. ed. CRC Press/Taylor and Francis.

Saffari, A., Daher, N., Ruprecht, A.A., De Marco, C., Pozzi, P., Boffi, R., Hamad, S.H., Shafer, M., Schauer, J.J., Westerdahl, D., Sioutas, C., 2014. Particulate Metals and Organic Compounds from Electronic and Tobacco-containing Cigarettes: Comparison of Emission Rates and Secondhand Exposure. Environ. Sci. Process. Impacts 2259–2267. doi:10.1039/C4EM00415A

Scheffler, S., Dieken, H., Krischenowski, O., Förster, C., Branscheid, D., Aufderheide, M., 2015. Evaluation of e-cigarette liquid vapor and mainstream cigarette smoke after direct exposure of primary human bronchial epithelial cells. Int. J. Environ. Res. Public Health 12, 3915–3925. doi:10.3390/ijerph120403915

Schoenborn, C., Gindi, R., 2015. Electronic cigarette use among adults: United States, 2014. Natl. Cent. Heal. Stat. 1–7.

Sleiman, M., Logue, J.M., Montesinos, V.N., Russell, M.L., Litter, M.I., Gundel, L.A., Destaillats, H., 2016. Emissions from Electronic Cigarettes: Key Parameters Affecting the Release of Harmful Chemicals. Environ. Sci. Technol. acs.est.6b01741.

doi:10.1021/acs.est.6b01741
Steenhof, M., Gosens, I., Strak, M., Godri, K.J., Hoek, G., Cassee, F.R., Mudway, I.S., Kelly, F.J., Harrison, R.M., Lebret, E., Brunekreef, B., Janssen, N.A.H., Pieters, R.H.H., 2011. In vitro toxicity of particulate matter (PM) collected at different sites in the Netherlands is associated with PM composition , size fraction and oxidative potential - the RAPTES project 1–15.
Surratt, J.D., Chan, A.W.H., Eddingsaas, N.C., Chan, M., Loza, C.L., Kwan, A.J., Hersey, S.P., Flagan, R.C., Wennberg, P.O., Seinfeld, J.H., Finlayson-Pitts, B.J., 2010. Reactive intermediates revealed in secondary organic aerosol formation from isoprene. Proc. Natl. Acad. Sci. 107, 6640–6645.
Wang, P., Chen, W., Liao, J., Matsuo, T., Ito, K., Fowles, J., Shusterman, D., Mendell, M., Kumagai, K., 2017. A Device-Independent Evaluation of Carbonyl Emissions from Heated Electronic Cigarette Solvents. PLoS One 12, e0169811. doi:10.1371/journal.pone.0169811
Williams, M., Villarreal, A., Bozhilov, K., Lin, S., Talbot, P., 2013. Metal and Silicate Particles Including Nanoparticles Are Present in Electronic Cigarette Cartomizer Fluid and Aerosol. PLoS One 8, 1–11. doi:10.1371/journal.pone.0057987
YahMezSoup, 2016. How long does your wicking last? [WWW Document]. URL https://www.reddit.com/r/Vaping/comments/465uir/how_long_does_your_wicking_last/ (accessed 5.10.17).
Zhang, H., Surratt, J.D., Lin, Y.H., Bapat, J., Kamens, R.M., 2011. Effect of relative humidity on SOA formation from isoprene/NO photooxidation: Enhancement of 2-methylglyceric acid and its corresponding oligoesters under dry conditions. Atmos. Chem. Phys. 11, 6411–6424. doi:10.5194/acp-11-6411-2011
Zhao, T., Shu, S., Guo, Q., Zhu, Y., 2016. Effects of design parameters and puff topography on heating coil temperature and mainstream aerosols in electronic cigarettes. Atmos. Environ. 134, 61–69. doi:10.1016/j.atmosenv.2016.03.027
Zhu, S.-H., Sun, J.Y., Bonnevie, E., Cummins, S.E., Gamst, A., Yin, L., Lee, M., 2014. Four hundred and sixty brands of e-cigarettes and counting: implications for product regulation. Tob. Control 23 Suppl 3, iii3-9. doi:10.1136/tobaccocontrol-2014-051670